A Macrocyclic Pyclen-Based Gd^{3+} Complex with High Relaxivity and pH Response

Juan C. Frías,[†] José Soriano,[‡] Salvador Blasco,[‡] Enrique García-España,[‡] Aurora Rodríguez-Rodríguez,[§] David Esteban-Gómez,[§] Fabio Carniato,[⊥] Mauro Botta,[⊥] Carlos Platas-Iglesias,*[,§] M Teresa Albelda*[,#]

[†] Departamento de Ciencias Biomédicas, Universidad CEU-Cardenal Herrera, CEU Universities, C/ Ramón y Cajal, s/n, 46115 Alfara del Patriarca, Valencia, Spain

[‡] Departamento de Química Inorgánica, Instituto de Ciencia Molecular, Universidad de Valencia, Edificio de Institutos de Paterna, Apdo 22085, 46071 Valencia, Spain

[§] Centro de Investigacións Científicas Avanzadas (CICA) and Departamento de Química, Universidade da Coruña, Campus da Zapateira-Rúa da Fraga 10, 15008 A Coruña, Spain

[⊥] Dipartimento di Scienze e Innovazione Tecnologica, Università del Piemonte Orientale "A. Avogadro", Viale T. Michel 11, 15121 Alessandria, Italy.

Departamento de Química Inorgánica, Universidad de Valencia, C/Dr. Moliner 50, 46100 Burjasot, Valencia, Spain.

ABSTRACT: We report the synthesis and characterization of the macrocyclic ligand 2,2'-((2-(3,9-bis(carboxymethyl)-3,6,9-triaza-1(2,6)-pyridinacyclodecaphane-6-yl)ethyl)azanediyl)diacetic acid (H_4L) and several of its complexes with the lanthanide ions. The structure of the free ligand was determined using X-ray diffraction measurements. Two N atoms of the pyclen moiety in *trans* position are protonated in the solid state, together with the exocyclic N atom and one of the carboxylate groups of the ligand. The relaxivity of the Gd^{3+} complex was found to increase from 6.7 mM^{-1} s^{-1} at pH 8.6 to 8.5 mM^{-1} s^{-1} below pH ~ 6.0. Luminescence lifetime measurements recorded from H_2O and D_2O solutions of the Eu^{3+} complex evidence the presence of a single complex species in solution at low pH (~5.0) that contains two inner-sphere water molecules. DFT calculations suggest that the coordination environment of the Ln^{3+} ion is fulfilled by the four N atoms of the pyclen unit, two oxygen atoms of the macrocyclic acetate groups and an oxygen atom of an exocyclic carboxylate group. The two inner-sphere water molecules complete coordination number nine around the metal ion. At high pH (~9.3) the lifetime of the excited $^5D_0$ level of Eu^{3+} displays a bi-exponential behavior that can be attributed to the presence of two species in solution with hydration numbers of $q = 0$ and $q = 1$. The ^1H NMR and DOSY spectra recorded from solutions of the Eu^{3+} and Y^{3+} complexes reveal a structural change triggered by pH and the formation of small aggregates at high pH values.

INTRODUCTION

Since the approval of $[Gd(DTPA)(H_2O)]^{2-}$ by the FDA in 1988 as the first contrast agent for clinical applications, hundreds of potential new contrast agents have been synthesized, although just a few of them are currently used on a daily basis in medicine. Most commercially available contrast agents are paramagnetic gadolinium complexes, which enhance the contrast of the image by shortening the magnetic relaxation time of the water protons in the surrounding tissues where they distribute. The efficiency of a paramagnetic complex to enhance the relaxation of water proton nuclei is generally characterized *in vitro* by its relaxivity, which normalizes the effect to a 1 mM concentration of the paramagnetic ion.[1–3]

The design of new contrast agents needs to fulfill some requirements such as: 1) thermodynamic and kinetic stability, a particularly important issue since the documentation of nephrogenic systemic fibrosis (NSF), an illness detected in patients with renal impairment after administration of certain contrast agents;[4–6] More recently gadolinium deposition in bones and brain of patients with normal renal function has been described.[4,7] 2) High relaxivity, which allows the use of lower doses of the contrast agent and the detection of low-concentration targets.[8,9] 3) Good solubility, as contrast agents are injected in rather large doses due to the low sensitivity of the technique.[8] 4) Rapid excretion to minimize the chances of complex dissociation and the consequent risk of deposition, and 5) Low osmolality and viscosity to avoid adverse reactions and necrosis of the tissue.[10]

Several strategies have been developed to achieve high relaxivities by optimizing the inner-sphere contribution to proton relaxivity.[11] The inner-sphere relaxivity is governed at the

magnetic fields used for clinical scanners (1.5 T and 3 T)[1] and biomedical research (usually up to 9.4 T)[1] by three main parameters: the mean residence time of coordinated water molecules in the Gd^{3+} coordination sphere (τ_M),[11,12] the rotational correlation time (τ_R)[13] and the number of water molecules directly coordinated to the metal ion (q).[2] The increase in q is generally achieved by decreasing the denticity of the ligand, which may result in a decreased complex stability. However, certain bis-hydrated complexes were found to present good stability profiles, sometimes comparable or even better than those of related $q = 1$ complexes.[14–19]

The toxicity of gadolinium(III) ions requires suitable chelating agents that provide thermodynamic stable and kinetically inert complexes.[8] This is usually achieved using open chain polyamines or polyazamacrocycles conveniently functionalized.[20] Pyridine-based macrocyclic ligands have shown to bind efficiently lanthanide (III) ions with the affinity being strongly affected by the ring size.[21,22] Twelve-membered rings with acetate or phosphonate side arms yield very stable complexes.[23–26] The pyridine in the macrocycle increases the stereochemical rigidity of the resulting complexes, a property often associated with an increase in their kinetic inertness.[8,24,27] The pyridine moiety may also provide a suitable site for a further functionalization,[28–30] which facilitates molecular recognition of specific targets. Furthermore, a bis-hydrated Gd^{3+} complex derived from pyclen containing α-functionalized acetate arms is currently under development as an extracellular MRI contrast agent, [31] as it presents a high relaxivity, remarkable kinetic inertness and a pharmacokinetic profile similar to those of commercially available contrast agents.[32]

Chart 1. Structures of the ligands discussed in this work.

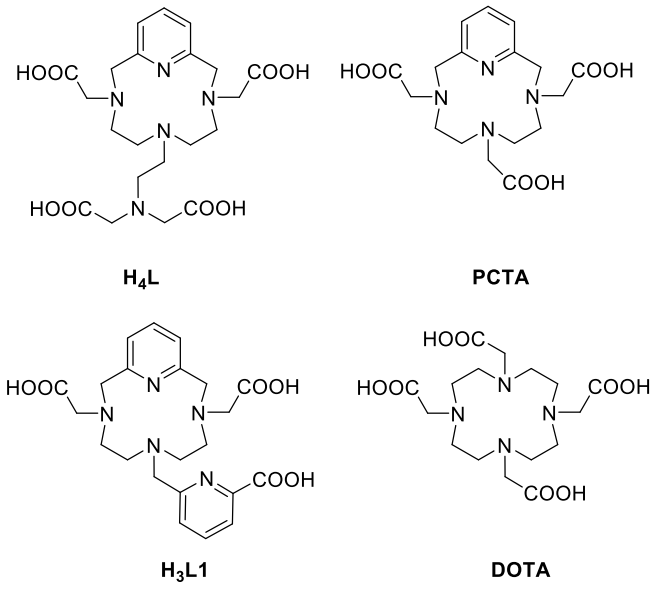

A huge amount of research in the field of MRI contrast agents has been devoted to develop systems that present response to relevant biochemical parameters, as for instance pH,[33–37] the concentration of biogenic cations[38–49] or neurotransmitters,[50–53] enzymatic activity[54–56] or redox potential.[57–63] Among these physiological parameters pH is considered to be an important biomarker of several diseases, including inflammatory processes and cancer.[64,65] Most pH-responsive Gd^{3+} agents contain a group coordinated to the metal ion (i. e. sulfonamide, amine, *p*-nitrophenol, phosphonate…) that is detached upon protonation close to physiological pH. This often results in an increased relaxivity associated with the increased number of water molecules in the first coordination sphere. Alternatively, pH response may be achieved by modulation of τ_R.[66]

Macrocyclic ligands based on the pyclen backbone such as PCTA (2,2′,2′′-[3,6,9,15-tetraazabicyclo[9.3.1]pentadeca-1(15),11,13-triene-3,6,9-triyl]triacetic acid)[67] and derivatives containing picolinate pendant arms replacing one or two of the acetate groups of PCTA (i. e. H_3L1, Chart 1) were found to form lanthanide complexes presenting interesting photophysical and relaxometric properties, including rather high stability constants, slow dissociation kinetics and high emission quantum yields of the Eu^{3+} and particularly Tb^{3+} complexes.[68,69] Herein we report a new derivative of PCTA and several of its lanthanide complexes. This new scorpiand macrocycle (denoted as H_4**L**, Chart 1) incorporates an iminodiacetate tail that may contribute to the coordination of lanthanide ions. We report the X-ray structure of the ligand, the physicochemical characterization of the Eu^{3+} complex and a full relaxometric study of the Gd^{3+} complex, which presents response to pH within the biologically relevant pH range. NMR and DFT studies were conducted to rationalize the unexpected relaxivity response to pH.

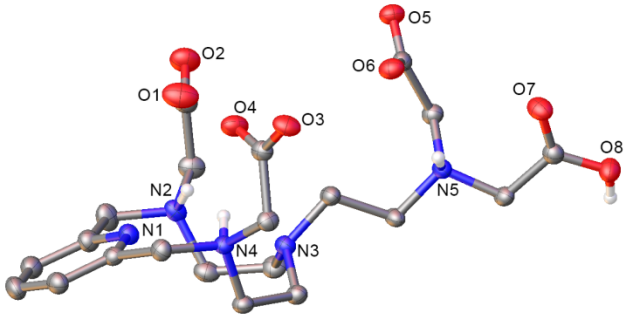

Figure 1. ORTEP representation of the $[H_4L]^{3+/3-}$ moiety. Ellipsoids represented at 50% probability.

RESULTS AND DISCUSSION

Ligand synthesis and characterization. The synthesis of the new pyridine-based contrast agent was carried out by a modification of the Richman-Atkins procedure where pertosylated tris(2-aminoethyl)amine (TREN-Ts) and 2,6-bis(bromomethyl)pyridine were refluxed in a 1:1 ratio in CH_3CN using K_2CO_3 as a base, following the procedure described previously.[70,71] Deprotection of the tosyl groups was achieved in acidic HBr/HAc media and phenol to obtain the hydrobromic salt. Later functionalization with potassium chloroacetate obtained from chloroacetic acid and potassium hydroxide afforded the tetra acetic acid derivative after column chromatography (DOWEX 1X8, formate form).

Crystals of H_4L suitable for X-ray diffraction were obtained by slow diffusion of ethanol into a solution of the ligand in water. The unit cell has a β angle very close to 90º, so initially

it was assumed to be orthorhombic. The structure could be solved in the Pmcn space group, but the result contained an unnatural mirror plane. A closer look revealed that the right space group was monoclinic $P2_1/c$ with $\beta = 90.009(3)$, and that the structure is a twin with two components which are mirrored to one another. The twin fraction was refined, the result being 0.476(1), which approximates to a perfect twin.

The asymmetric unit contains one unit of the ligand L along with a number of water molecules. The molecule of L contains a total of four protons, since it had been synthesized as H_4L and no other atoms are present in the crystal except solvent molecules. Three of those protons were found in the Fourier map on nitrogen atoms N2, N4 and N5 (Figure 1). The location of the fourth proton was decided by analyzing bond lengths of the carboxylate moieties and located on O8 (Figure S1, Supporting Information). This means that the H_4L moiety holds a total of six charges; three positive (on N2, N4 and N5) and three negative (on carboxylates C15, C17 and C19). The three charged carboxylates are oriented towards the same side of the molecule (see Figure 1) and all three of them contain an intramolecular hydrogen bond with the nearest protonated nitrogen (see Table S1, Supporting Information), while at the same time they form a rich hydrogen bond network with a number of water molecules (see Figure S2, Supporting Information). The protonated carboxylate also forms hydrogen bonds with both a water molecule and the same group of a neighbor $H_4L^{3+/3-}$ entity. In addition to hydrogen bond interactions, electrostatic forces seem to play an important role in the packing. Molecules of $H_4L^{3+/3-}$ pack with each other along an antiparallel orientation with their neighbors in such a manner that positive and negative charges are aligned (see Figure S3, Supporting Information).

The protonation of the two amine N atoms of the macrocyclic unit in *trans* position (N2 and N4) is in agreement with the macroscopic protonation sequence established by NMR measurements for PCTA and closely related derivatives, which indicated that the first protonation of the macrocycle occurs at the N atom in *trans* position with respect to the pyridyl N atom, as also observed in the solid state for the monoprotonated form of pyclen.[72] However, the second protonation step provokes a shift of the former proton to afford a bis-protonated species on the two *trans* amine N atoms adjacent to N3.[24]

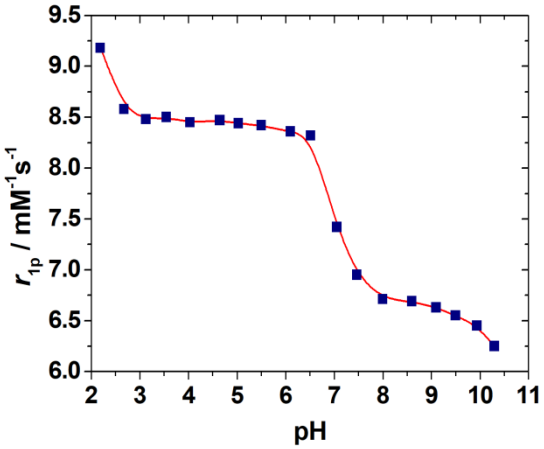

Figure 2. Plot of the ^{1}H relaxivity (20 MHz, 25 °C) of GdL as a function of pH.

Proton relaxivity. The relaxivity (r_{1p}) of $[GdL]^-$ was first investigated at 25 ºC and 20 MHz over a wide pH range (ca. 10 to 2). Relaxivity takes a value of 6.7 mM^{-1} s^{-1} at pH 8.6, while below pH 8.0 increases reaching a value of 8.5 mM^{-1} s^{-1}. This represents a 1.8-fold increase of proton relaxivity on decreasing pH. Relaxivity remains constant in the pH range ~ 6.0 -3.0, indicating that the complex does not dissociate within this pH range. The relaxivity observed within the pH range 6.0 -3.0 is very similar to that observed for pyclen-based bis-aquated complexes with similar molecular weight.[73] Below pH 3.0, relaxivity increases as a result of complex dissociation. A noticeable decrease of r_{1p} is also observed above pH 9.0, an effect that can be attributed to the formation of hydroxo species, as suggested for different Gd^{3+} complexes[74] including PCTA derivatives.[21,75] The analysis of the r_{1p} vs pH profile provides a pK_a of 7.01 $\pm$ 0.03, which must be related to the protonation of the amine nitrogen atom of the iminodiacetate group, as protonation of the macrocyclic N atoms should cause complex dissociation. These results together with the hydration numbers obtained from luminescence lifetime measurements (see below) point to a change in the hydration number of the complex, from 1 at pH > 8.0 to 2 at pH < 6.0, triggered by the protonation of the ligand.

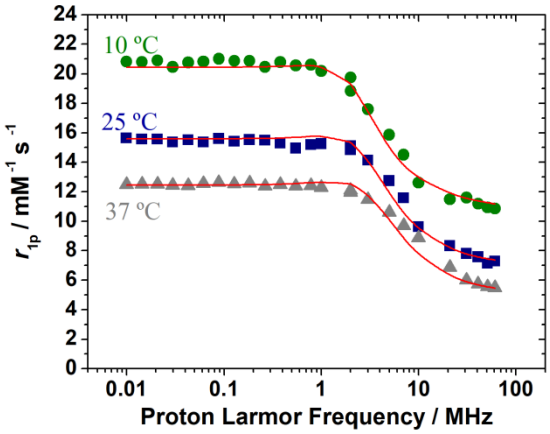

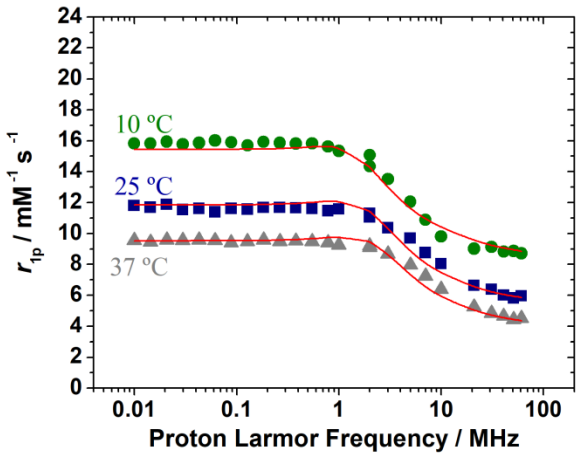

Figure 3. ^{1}H Nuclear Magnetic Relaxation Dispersion (NMRD) profiles of GdL recorded at pH 4.98 (top) and 9.20 (bottom). The solid lines represent the fits of the data as explained in the text.

Nuclear magnetic relaxation dispersion profiles (NMRD) were recorded at pH values of 4.98 and 9.20 to gain additional insight into the parameters that control the relaxivity of the [Gd**L**]$^{-}$ and [GdH**L**] species (Figure 3). NMRD profiles were recorded at three different temperatures (10, 25 and 37 ºC) covering magnetic field strengths of 2.3×10^{-4} to 1.1 T, which correspond to proton Larmor frequencies of 0.01-60 MHz. The relaxivities recorded at both pH values decrease with increasing temperature, indicating that the fast rotation of the complexes in solution limits r_{1p}. This is typical of small Gd^{3+} complexes with short rotational correlation times (τ_R) and fast water exchange rates.[76] The relaxivities recorded at pH 4.98 are higher than those measured at high pH over the whole range of proton Larmor frequencies, which is in line with an increased hydration of the protonated form of the complex.

Photophysical properties and hydration number. The emission spectra of the Eu^{3+} complex of L were recorded at two different pH values (4.5and 9.5) to gain information on the relaxometric behavior of the Gd^{3+} analogue. The emission spectra, recorded under excitation through the pyridyl chromophore at 273 nm, present the $^{5}D_0 \rightarrow {}^{7}F_J$ transitions typical of Eu^{3+} (Figure 4).[77] The emission spectra show a single $^{5}D_0 \rightarrow {}^{7}F_0$ transition at 578.4 nm and three components for the $^{5}D_0 \rightarrow {}^{7}F_1$ transition at 587.8, 591.0 and 596.6 (pH 4.5) and 588.0, 591.0 and 595.8 nm. The shape of the emission spectra does not change very much with pH, the main differences being noticed for the intensity and splitting of the $^{5}D_0 \rightarrow {}^{7}F_2$ transition. The intensity of the latter transition is very sensitive to changes in the coordination environment, while the intensity of the $^{5}D_0 \rightarrow {}^{7}F_1$ transition is relatively independent of the coordination environment due to its magnetic dipole character.[78] Increasing the pH results in a noticeable increase of the intensity of the $^{5}D_0 \rightarrow {}^{7}F_2$ transition with respect to the $^{5}D_0 \rightarrow {}^{7}F_1$ one, which signals a change in the metal coordination environment likely related to the coordination of more polarizable donor groups.[79,80] This suggests that inner-sphere water molecules are replaced by more polarizable carboxylate donor atoms upon increasing the pH.[81]

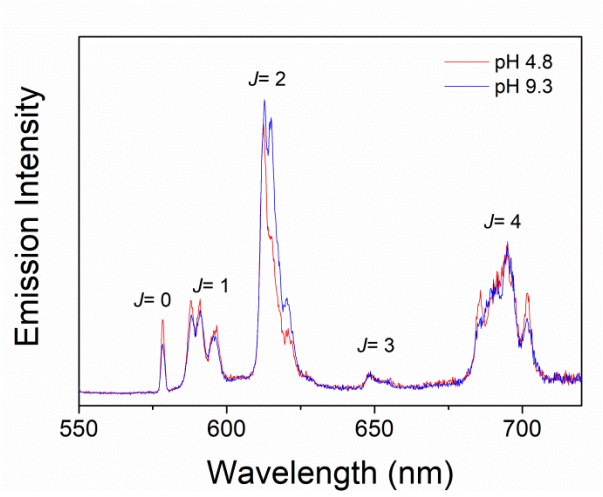

Figure 4. Emission spectra of the Eu^{3+} recorded at different pH values (5×10^{-5} M, λ_{exc} = 273 nm).

The decay profile of the $^{5}D_0$ excited state measured in H_2O solution at pH 4.8 can be perfectly fitted to a monoexponential function with a lifetime of 0.384 ms, which is typical of Eu^{3+} complexes containing two coordinated water molecules.[82] This suggests the presence of a single Eu^{3+} site in solution (Table 1, Figure 5). The emission lifetime recorded at the same pH in D_2O solution is considerably longer (2.126 ms). The lifetimes recorded in H_2O and D_2O solutions afford hydration numbers close to 2.0 using the methods proposed by Horrocks[83] and Beeby,[84] indicating the presence of two water molecules directly coordinated to the metal ion. Conversely, the emission lifetimes recorded at pH 9.3 cannot be fitted with monoexponential decay functions (Figure 5). The lifetimes determined in H_2O by bi-exponential fitting of the data point to the presence of a minor component (30%) with a short lifetime of 0.290 ms and a major component with a longer lifetime of 0.683 ms. Measurements in D_2O solution show that the emission lifetime of the species with the short lifetime is only marginally affected by solvent deuteration, which provides q = 0 within experimental error (Table 1). The emission lifetimes of the major component recorded in H_2O and D_2O solutions afford q values close to 1 (0.7 – 0.8), suggesting that the main species present in solution contains one coordinated water molecule.

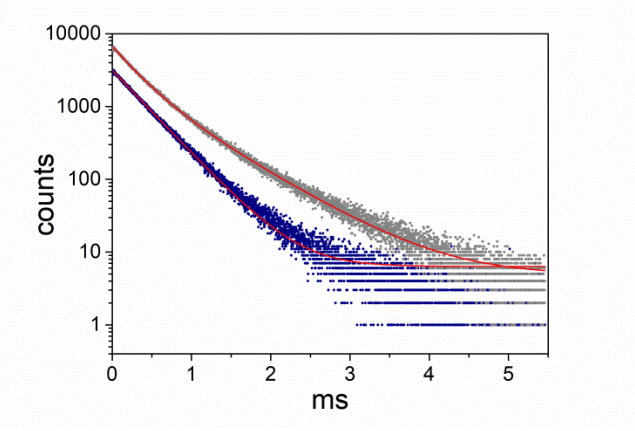

Figure 5. Emission decay profiles recorded in H_2O solutions of the Eu^{3+} complex at different pH values (5×10^{-5} M, λ_{exc} = 273 nm, λ_{em} = 613 nm). The red lines correspond to the fit of the data according to single (pH = 4.8) and double (pH 9.3) exponential decay functions.

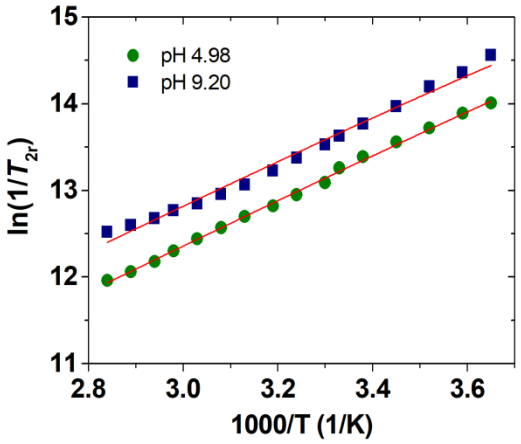

Figure 6. Temperature dependence of the reduced ^{17}O transverse relaxation rates measured at 11.75 T (9.4 mM). The solid lines through the data points were calculated with the parameters shown in Table 2.

Table 1. Relative intensities of the $^5D_0 \rightarrow {}^7F_J$ transitions (J = 1 and 2), luminescence lifetimes and hydration numbers of the Eu^{3+} complex recorded at different pH values.[a]

	$\Delta J = 1$ / $\Delta J = 2$	τ_{H_2O} / ms	τ_{D_2O} / ms	q
pH 4.5	0.50	0.380(4)	2.126(1)	2.3[b] /2.1[c]
pH 9.5	0.36	τ_1 = 0.290(2) (30%)	τ_1 = 0.320(2) (15%)	0.1[b] /0.0[c]
		τ_2 = 0.683(9) (70%)	τ_2 = 1.766(3) (85%)	0.8[b] /0.7[c]

[a] Eu^{3+} concentration 5×10^{-5}, λ_{exc} = 273 nm, λ_{em} = 613 nm. [b] Determined according to ref [84]. [c] Determined according to ref [83].

Table 2. Parameters obtained from the simultaneous analysis of ^{17}O NMR and ^1H NMRD data.

	GdL (pH 4.98)	**GdL (pH 9.20)**	**GdPCTA** [b]	**GdDOTA** [c]
r_{1p} at 25/37 ºC / mM^{-1} s^{-1} [b] (20 MHz)	8.3/6.9	6.7/5.2	6.9/ *d*	4.7/3.8
$k_{ex}^{298}/10^6$ s^{-1}	131 ± 1.3	84 ± 0.8	14.3	4.1
$\Delta H^{\ddagger}$ / kJ mol^{-1}	19.1 ± 1.3	18.8 ± 1.5	45	49.8
τ_R^{298} / ps	85 ± 4	122 ± 5	70	77
E_r / kJ mol^{-1}	20.7 ± 1.3	20.9 ± 1.1	*d*	16.1
τ_v^{298}/ ps	80 ± 5	106 ± 6.0	28	11
E_v / kJ mol^{-1}	1.0[a]	1.0[a]	3.6	1.0[a]
D_{GdH}^{298} / 10^{-10} m^2 s^{-1}	22.4[a]	22.4[a]	22.4[a]	22
E_{DGdH}/ kJ mol^{-1}	20[a]	20[a]	*d*	20.2
Δ^2 / 10^{19} s^{-2}	1.06 ± 0.3	0.69 ± 0.2	2.8	1.6
$A/\hbar$ / 10^6 rad s^{-1}	-3.8[a]	-3.8[a]	-3.8[a]	-3.7
r_{GdH} / Å	3.1[a]	3.1[a]	3.1[a]	3.1[a]
a_{GdH} / Å	3.8[a]	3.8[a]	3.8[a]	3.5[a]
q^{298}	2[a]	1[a]	2[a]	1[a]

[a] Parameters fixed during the fitting procedure. [b] Data from reference [85]. [c] Data from reference [86]. [d] Not reported.

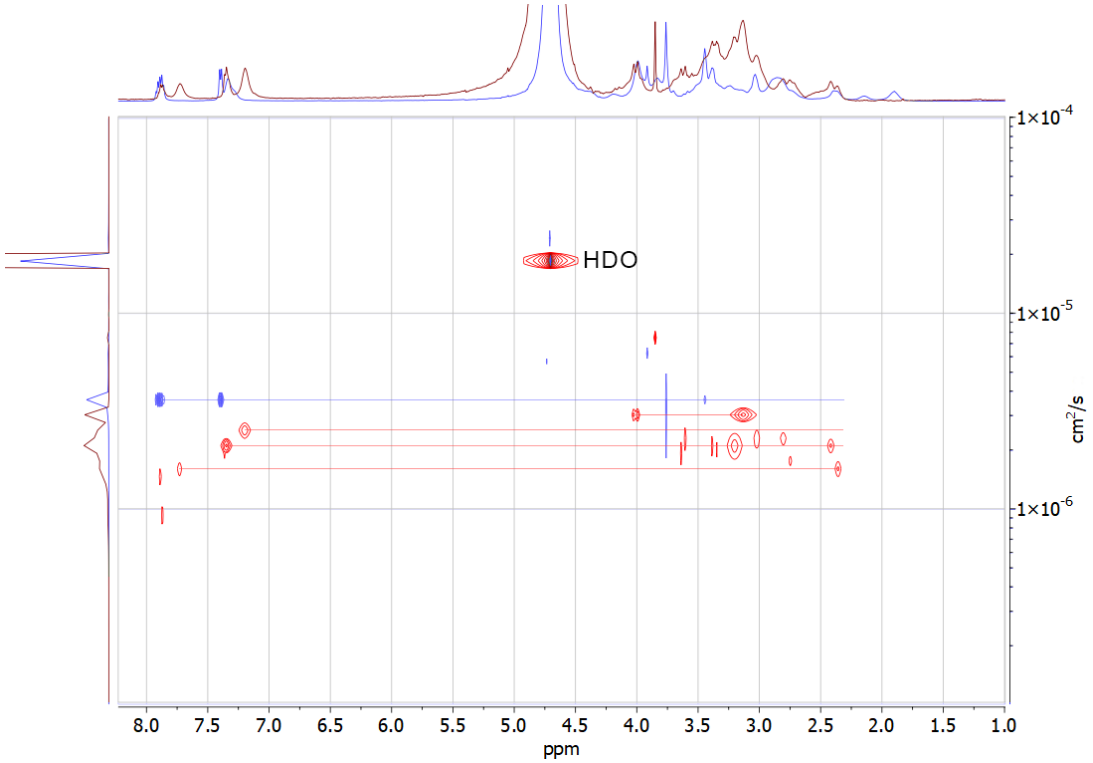

Figure 7. Superposed ^{1}H DOSY (D_2O, 500 MHz, 298 K) experiments of YL recorded at pH 5.0 (blue) and 9.0 (red).

^{17}O NMR studies and parameters determining r_{1p}. The observed relaxivities depend upon a relatively large number of parameters, and thus it is important to obtain information about some of them using independent techniques.[87] We therefore measured ^{17}O NMR transverse relaxation rates, which provide direct information on the exchange rate of the coordinated water molecules. The reduced transverse relaxation rates present an almost linear variation with the inverse temperature (Figure 6). The positive slope indicates that the system is in the fast exchange regime over the whole range of accessible temperatures, pointing to a fast water exchange.[88,89]

A simultaneous fit of the ^{1}H NMRD profiles and ^{17}O NMR relaxation data was carried out to estimate the parameters governing relaxivity both at high and low pH. The analysis of the data was performed by fixing some parameters to reasonable values: 1) The distance between the proton nuclei of coordinated water molecules and the Gd^{3+} ion was fixed to 3.1 Å following previous NMRD and ENDOR studies;[86,90] 2) The distance of closest approach of a second sphere water molecule, which affects the outer-sphere contribution to relaxivity, was fixed at 3.8 Å;[91] 3) The diffusion coefficient D_{GdH}^{298} and its activation energy E_{DGdH} were fixed to reasonable values of ($D_{H_2O}^{298}$ = 22.4 × 10^{-10} m^2 s^{-1} and E_{DH2O} = 20 kJ mol^{-1};[92] 4) The activation energy for the modulation of the zero-field splitting energy was set to 1 kJ mol^{-1};[86,93] 5) The value for the ^{17}O scalar hyperfine coupling constant ($A/\hbar$), which was shown to be little affected by the nature of the ligand coordinated to Gd^{3+}, was fixed to the standard value of -3.8 ×10^6 rad s^{-1};[94,95] 6) Finally, the number of water molecules coordinated to the Gd^{3+} ion was fixed to q = 2 at pH 4.98 and q = 1 at pH 9.20 on the grounds of the hydration numbers determined for the Eu^{3+} analogue from luminescence lifetime measurements. At high pH luminescence measurements indicate the presence of at least two species in solution with different hydration numbers, with the major species being that with q = 1. Thus, the results of the fits of ^{1}H and ^{17}O relaxation data at high pH need to be taken with some care.

The ^{17}O NMR relaxation data and ^{1}H NMRD profiles could be fitted well with the parameters shown in Table 2. The water exchange of the coordinated water molecules is rather fast, particularly at pH 4.98. At this pH k_{ex}^{298} is one order of magnitude faster than for the bis-hydrated GdPCTA complex,[85] and more than 30 times faster than for GdDOTA.[86] The water exchange rate is somewhat reduced at pH 9.2, but remains very high. The value of τ_R obtained at low pH is very similar to those reported for GdPCTA and GdDOTA, which are expected to present similar hydrodynamic radii. At high pH τ_R is longer, which suggests a certain degree of aggregation in solution (see below). Finally, the parameters that define the relaxation of the electron spin: The mean square zero-field-splitting energy (Δ^2) and its correlation time (τ_v), take values comparable to those determined for Gd^{3+} complexes of PCTA and DOTA derivatives (Table 2).

NMR and DFT studies. ^{1}H NMR studies were carried out using solutions of the diamagnetic Y^{3+} complex at pH values of 5.0 and 9.0. The ionic radii and coordination chemistry of Gd^{3+} and Y^{3+} are very similar, and thus Y^{3+} complexes can be used as diamagnetic subrogates of the Gd^{3+} analogues.[96] The spectrum recorded at pH 5.0 is reasonably well resolved, and shows three signals for the aromatic proton nuclei of the pyridyl unit at 7.89, 7.39 and 7.33 ppm. The signals due to aliphatic proton nuclei are observed in the range 1.8-4.4 ppm

and are relatively broad at room temperature. Diffusion Ordered Spectroscopy (DOSY) experiments show that all ^{1}H NMR signals resonate along a single diffusion value of 3.63×10^{-10} m^2 s^{-1} (Figure 7). This diffusion coefficient is similar to those determined previously in D_2O solution for small lanthanide complexes displaying discrete structures in solution. The use of the Stokes–Einstein equation for translation provides a van der Waals radius of 5.49 Å.

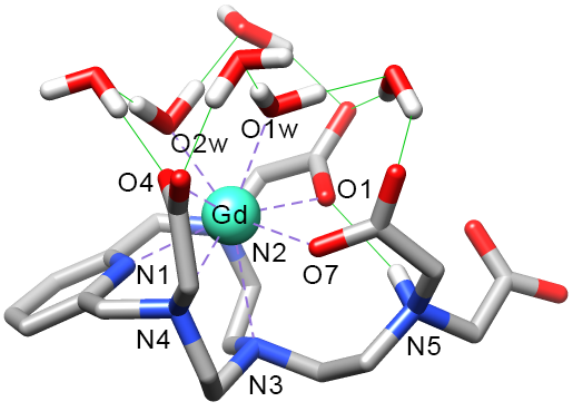

Figure 8. Optimized geometry of [GdHL] obtained with DFT calculations. Hydrogen atoms attached to carbon atoms are omitted for simplicity.

DFT calculations were carried out to gain information on the structure of the Gd^{3+} complex of L upon protonation (see computational details below). The model system used included two inner-sphere water molecules, in line with the results obtained from luminescence and relaxometric data. Four explicit second-sphere water molecules were also included in the model to improve the description of the Gd-O_{water} bonds, following previous computational studies.[97] Given that GdPCTA derivatives are known to contain two inner-sphere water molecules, it is reasonable to assume that a donor atom of the iminodiacetate group coordinates to the metal ion, as otherwise a higher hydration number would be expected (i. e. GdPC2A shows a higher hydration number than GdPCTA).[67] Complex protonation (pK_a = 7.01, see above) must occur at the amine N atom of the iminodiacetate group. Our DFT calculations provide a minimum energy structure that is in line with this reasoning (Figure 8). The metal ion is coordinated to the four N atoms of the macrocyclic fragment, two oxygen atoms of the acetate groups and two oxygen atoms of two inner-sphere water molecules (Table S2, Supporting Information). Nine-coordination is completed by an oxygen atom of the iminodiacetate moiety. The protonated N atom of the iminodiacetate group is involved in hydrogen bond interactions with two oxygen atoms of carboxylate groups. A similar coordination was suggested for a DO3A derivative containing a protonated aminophosphonate group on the basis of spectroscopic studies.[98]

The molecular volume of the $[GdHL(H_2O)_2]\cdot4H_2O$ system, estimated as the volume inside a contour of 0.001 electron Bohr^{-3} of the electron density, is 729.5 Å^3. The radius of the complex can be estimated to be 5.24 Å considering a sphere of the same volume. This value is in excellent agreement with the one estimated from the measured diffusion coefficient (5.49 Å), confirming the discrete nature of the complex in solution.

The ^{1}H NMR spectrum of the Y^{3+} complex recorded at pH 9.0 is more complex than that recorded at low pH (Figure 8). The aliphatic region is poorly resolved, while four signals are clearly observed for the three proton nuclei of the pyridyl ring, which evidences the presence of more than one complex species in solution. The corresponding DOSY spectrum reveals the presence of four major species with diffusion coefficients of 3.04×10^{-10} m^2 s^{-1}, 2.53×10^{-10} m^2 s^{-1}, 2.10×10^{-10} m^2 s^{-1} and 1.60×10^{-10} m^2 s^{-1}, which correspond to van der Waals radii of 6.55, 7.87, 9.49 and 12.45 Å. These results suggest that at basic pH the complex forms small aggregates in solution, presumably due to intermolecular coordination of the iminodiacetate group. This intermolecular coordination reduces the number of water molecules coordinated to the metal ion, yielding q = 0 and q = 1 species, as suggested by luminescence lifetime measurements. Coordination of the negatively charged iminodiacetate unit is also consistent with the spectral changes observed in the emission spectra of the Eu^{3+} complex upon increasing pH. A few examples of Ln^{3+} complexes that form stable aggregates in solution assembled through bridging carboxylate units have been reported in the literature.[99–101] The formation of these aggregates does not cause loss of pH-dependency of relaxivity, as reported recently for GdDO3A-arylsulfonamide complexes.[102]

CONCLUSIONS

In summary, we have reported a Gd^{3+} complex with an interesting relaxivity pH response associated with a change in the number of water molecules coordinated to the metal ion. The protonation of the complex occurs in the biologically relevant 6.0–8.0 pH range, and involves the exocyclic N atom of the ligand. DFT and spectroscopic studies suggest that at low pH the iminodiacetate moiety of the ligand remains coordinated to the Ln^{3+} ion through one of the carboxylate oxygen atoms. Upon deprotonation, the iminodiacetate unit allows intermolecular coordination and formation of small aggregates, resulting in a reduced hydration number. The results reported in this paper represent one of the few examples of Ln^{3+} complexes for which the formation of stable aggregates in solution has been established. However, it is likely that many other coordinatively unsaturated Ln^{3+} complexes also undergo aggregation in solution, suggesting that this possibility must be considered with much more caution than is usually taking at the moment.

EXPERIMENTAL AND COMPUTATIONAL SECTION

Materials. 2-(3,6,9-Triaza-1(2,6)-pyridinacyclodecaphane-6-yl)ethan-1-amine (PYTREN) was synthesized as described previously.[70,71] All other reagents and solvents were purchased from commercial sources and used without further purification.

Spectroscopic studies. The ^{1}H and ^{13}C NMR spectra of the ligand and intermediates were recorded on a Bruker Advance DRX 300 spectrometer operating at 300 MHz for ^{1}H and at 75.4 MHz for ^{13}C. MS analysis was performed under ESI conditions on a LCT Premier mass spectrometer. The Eu^{3+},

Gd^{3+} and Y^{3+} complexes were prepared by mixing stoichiometric amounts of $LnCl_3 \cdot 6H_2O$ with an aqueous solution of the ligand while maintaining the pH at 6 by addition of 1 M NaOH. The pH of the final solutions was adjusted with diluted HCl and NaOH solutions. ^1H NMR spectra of the Eu^{3+} complex were recorded on a Bruker Avance III spectrometer operating at 300 MHz for ^1H. DOSY spectra of the Y^{3+} complex were recorded using a Bruker Avance 500 MHz spectrometer equipped with a dual $^1H/^{13}C$ cryoprobe. The ^1H $1/T_1$ NMRD profiles were obtained with a fast field-cycling Stelar SmartTracer relaxometer (Mede, Pavia, Italy) varying the magnetic field strength from 0.00024 to 0.25 T, which corresponds to proton Larmor frequency range of 0.01-10 MHz. The instrument operates under computer control providing $1/T_1$ values with an absolute uncertainty of ± 1%. Temperature was controlled with a Stelar VTC-91 airflow heater equipped with a calibrated copper–constantan thermocouple (uncertainty of ±0.1 K). Additional data at higher field (20-60 MHz) were obtained using a Stelar Relaxometer coupled to a Bruker WP80 NMR electromagnet reconditioned for variable-field measurements (15-80 MHz proton Larmor frequency). The concentration of the complex was determined using Bulk Magnetic Susceptibility (BMS) shift measurements performed at 11.7 T. ^{17}O NMR spectra were acquired on a Bruker Avance III spectrometer (11.7 T) using a 5 mm probe and standard temperature control. An aqueous solution of the complexes (9.4 mM) was enriched to reach 2.0% of the ^{17}O isotope (Cambridge Isotope). The transverse relaxation rates were measured from the signal width at half-height.

Excitation and emission spectra in the UV−vis region were obtained with a Horiba FluoroMax Plus-P spectrofluorometer equipped with a 150 W ozone-free xenon arc lamp and a R928P photon counting emission detector, as well as a photodiode reference detector for monitoring lamp output. All spectra were corrected for the instrumental response. An integration time of 0.1 s was used in all steady state measurements. Luminescence decays were measured using the Time-Correlated Single Photon Counting (TCSPC) module of the same instrument using a xenon flash lamp.

2,2'-((2-(3,9-Bis(carboxymethyl)-3,6,9-triaza-1(2,6)-pyridinacyclodecaphane-6-yl)ethyl)azanediyl)diacetic acid (H_4L). Chloroacetic acid (11.7 mmol) and KOH (11.7 mmol) were added to an aqueous solution of 2-(3,6,9-triaza-1(2,6)-pyridinacyclodecaphane-6-yl)ethan-1-amine (PYTREN, 2.6 mmol) at pH 10 adjusted with 0.1 M KOH. The mixture was refluxed for 24 hours. After 24 hours the mixture was cooled down at room temperature and then the solution neutralized with KOH. The solution was concentrated and loaded onto an ion-exchange resin (Dowex 1x8-400). The column was washed with H_2O and the product was eluted with a 0.02M formic acid solution to afford a white solid product. ^1H NMR (D_2O, 300 MHz): δ_H 2.89 (bs, 4H), 3.07 (bm, 2H), 3.51 (bm, 6H), 3.95 (s, 4H), 4.13 (s, 4H), 4.82 (s, 4H), 7.45 (d, ^3J=7.5 Hz, 2H), 7.96 (t, ^3J=7.5 Hz, 1H). ^{13}C NMR (D_2O, 75 MHz): δ_C 56.4, 57.6, 61.9, 65.5, 65.9, 68.1, 68.4, 131.2, 131.6, 148.6, 158.2, 178.1, 178.2. HRMS: *m/z* calcd for $C_{21}H_{30}N_5O_8$ 480.2100; found 480.2109. MS-ES: *m/z* 482 ($M + H^+$); 504.2 ($M + Na^+$).

Crystal structure determination. 0.1 mmol of H_4L were dissolved in pure water and ethanol vapor was diffused into the vessel. Colorless crystals suitable for X-ray diffraction were obtained were obtained after four days. The crystals were measured in a Bruker D8 Venture X-ray diffractometer using MoKα radiation (λ= 0.71073Å) equipped with an Oxford low temperature unit operating at 130 K. Indexing, strategy and data collection were performed with APEX3 software suite. OLEX2 was used as frontend for solving and refining.[103] The initial structure was solved with direct methods using SIR2014.[104] The resulting structure was refined with SHELXL2014.[105] Initially, an isotropic refinement was performed on the non-hydrogen atoms and then anisotropic refinement was introduced. Hydrogen atoms H2, H4 and H5 which are the ones placed onto nitrogen atoms, were found in the Fourier map and their positions were left free in the refinement. The rest of hydrogen atoms were placed in calculated positions. Two soft restraints were placed to orient properly water moieties containing O10 and O12. Crystal data and structure refinement details: Formula: $C_{21}H_{31}N_5O_8 \cdot 4.272H_2O$; MW: 558.34; crystal system: monoclinic; space group: $P2_1/c$; a=14.7386(14) Å; b=13.7004(13) Å; c=12.9591(11) Å; β=90.009(3)°; V=2616.8(4) Å^3; $F(000)$=1195; Z=4; D_{calc}=1.420 g cm^{-3}; μ=0.117 mm^{-1}; θ range=2.57– 28.20°; R_{int}=0.0910; 52998 measured reflections, of which 5422 were independent and 6544 were unique with $I > 2\sigma(I)$. GOF on F^2=1.037; $R1$=0.0422; $wR2$ (all data) = 0.1042; Largest differences peak and hole: 0.210 and –0.259 eÅ^{-3}.

DFT calculations. All DFT calculations were carried out by using the Gaussian 09 package (Revision E.01)[ref] within the hybrid meta-GGA approximation with the TPSSh exchange-correlation functional.[106,107] Solvent effects were included using the integral-equation formalism variant of the polarizable continuum model (IEFPCM).[108] The 6–31G(d,p) basis set was used for C, H, N and O, while Gd was described with the large-core quasi-relativistic effective core potential approximation and the associated [5s4p3d]-GTO valence-basis set.[109] Geometry optimizations were followed by frequency calculations to confirm the nature of the optimized geometries as local minima.

ASSOCIATED CONTENT

Supporting Information

The Supporting Information is available free of charge on the ACS Publications website at DOI: XXXXX. Additional crystallographic and DFT data (PDF).

Accession codes

CCDC 1884191 contains the supplementary crystallographic data for this paper. These data can be obtained free of charge via www.ccdc.cam.ac.uk/data_request/cif, or by emailing data_request@ccdc.cam.ac.uk, or by contacting The Cambridge Crystallographic Data Centre, 12 Union Road, Cambridge CB2 1EZ, UK; fax: +44 1223 336033.

AUTHOR INFORMATION

Corresponding Authors

*E-mail: carlos.platas.iglesias@udc.es (C. P.-I)
*E-mail: teresa.albelda@uv.es (M. T. A.)

ORCID

Juan C. Frías: 0000-0002-2948-5086
Salvador Blasco: 0000-0002-8142-8337
Enrique García-España: 0000-0002-4601-6505
David Esteban-Gómez: 0000-0001-6270-1660
Mauro Botta: 0000-0003-4192-355X
Carlos Platas-Iglesias: 0000-0002-6989-9654
M. Teresa Albelda: 0000-0002-9572-8912

Author Contributions

The manuscript was written through contributions of all authors. All authors have given approval to the final version of the manuscript.

Notes

The authors declare no competing financial interest.

ACKNOWLEDGMENT

Authors A. R.-R., D. E.-G. and C. P.-I. thank Ministerio de Economía y Competitividad (CTQ2016-76756-P) and Xunta de Galicia (ED431B 2017/59 and ED431D 2017/01) for generous financial support, and Centro de Supercomputación of Galicia (CESGA) for providing the computer facilities. M.B. and F.C. thank Università del Piemonte Orientale for financial support (FAR 2019).

REFERENCES

(1) **Wahsner, J.; Gale, E. M.; Rodríguez-Rodríguez, A.; Caravan, P. Chemistry of MRI Contrast Agents: Current Challenges and New Frontiers. *Chem. Rev.* 2019, *119* (2), 957–1057.**

(2) **Caravan, P.; Ellison, J. J.; McMurry, T. J.; Lauffer, R. B. Gadolinium(III) Chelates as MRI Contrast Agents: Structure, Dynamics, and Applications. *Chem. Rev.* 1999, *99* (9), 2293–2352.**

(3) ***The Chemistry of Contrast Agents in Medical Magnetic Resonance Imaging, Second Edition*, 2nd Edn.; Merbach, A., Helm, L., Tóth, É., Eds.; WILEY, 2013.**

(4) **Layne, K. A.; Dargan, P. I.; Archer, J. R. H.; Wood, D. M. Gadolinium Deposition and the Potential for Toxicological Sequelae – A Literature Review of Issues Surrounding Gadolinium-Based Contrast Agents. *Br. J. Clin. Pharmacol.* 2018, *84* (11), 2522–2534.**

(5) **Grobner, T. Gadolinium - A Specific Trigger for the Development of Nephrogenic Fibrosing Dermopathy and Nephrogenic Systemic Fibrosis? *Nephrol. Dial. Transplant.* 2006, *21* (4), 1104–1108.**

(6) **Marckmann, P.; Skov, L.; Rossen, K.; Dupont, A.; Damholt, M. B.; Heaf, J. G.; Thomsen, H. S. Nephrogenic Systemic Fibrosis: Suspected Causative Role of Gadodiamide Used for Contrast-Enhanced Magnetic Resonance Imaging. *J. Am. Soc. Nephrol.* 2006, *17* (9), 2359–2362.**

(7) **Kanal, E.; Tweedle, M. F. Residual or Retained Gadolinium: Practical Implications for Radiologists and Our Patients. *Radiology* 2015, *275* (3), 630–634.**

(8) **Clough, T. J.; Jiang, L.; Wong, K. L.; Long, N. J. Ligand Design Strategies to Increase Stability of Gadolinium-Based Magnetic Resonance Imaging Contrast Agents. *Nat. Commun.* 2019, *10* (1420), 1–14.**

(9) **Terreno, E.; Castelli, D. D.; Viale, A.; Aime, S. Challenges for Molecular Magnetic Resonance Imaging. *Chem. Rev.* 2010, *110* (5), 3019–3042.**

(10) **Hao, D.; Ai, T.; Goerner, F.; Hu, X.; Runge, V. M.; Tweedle, M. MRI Contrast Agents: Basic Chemistry and Safety. *J. Magn. Reson. Imaging* 2012, *36* (5), 1060–1071.**

(11) **Caravan, P.; Esteban-Gómez, D.; Rodríguez-Rodríguez, A.; Platas-Iglesias, C. Water Exchange in Lanthanide Complexes for MRI Applications. Lessons Learned over the Last 25 Years. *Dalt. Trans.* 2019, *48* (30), 11161–11180.**

(12) **Sherry, A. D.; Wu, Y. The Importance of Water Exchange Rates in the Design of Responsive Agents for MRI. *Curr. Opin. Chem. Biol.* 2013, *17* (2), 167–174.**

(13) **Caravan, P.; Farrar, C. T.; Frullano, L.; Uppal, R. Influence of Molecular Parameters and Increasing Magnetic Field Strength on Relaxivity of Gadolinium- and Manganese-Based T1 Contrast Agents. *Contrast Media Mol. Imaging* 2009, *4* (2), 89–100.**

(14) **Gale, E. M.; Kenton, N.; Caravan, P. [Gd(CyPic3A)(H2O)2]-: A Stable, Bis(Aquated) and High-Relaxivity Gd(III) Complex. *Chem. Commun.* 2013, *49* (73), 8060–8062.**

(15) **Messeri, D.; Lowe, M. P.; Parker, D.; Botta, M. A Stable, High Relaxivity, Diaqua Gadolinium Complex That Suppresses Anion and Protein Binding. *Chem. Commun.* 2001, *1* (24), 2742–2743.**

(16) **Aime, S.; Calabi, L.; Cavallotti, C.; Gianolio, E.; Giovenzana, G. B.; Losi, P.; Maiocchi, A.; Palmisano, G.; Sisti, M. [Gd-AAZTA]-: A New Structural Entry for an Improved Generation of**

MRI Contrast Agents. *Inorg. Chem.* 2004, *43* (24), 7588–7590.

(17) Baranyai, Z.; Uggeri, F.; Giovenzana, G. B.; Bényei, A.; Brücher, E.; Aime, S. Equilibrium and Kinetic Properties of the Lanthanoids(III) and Various Divalent Metal Complexes of the Heptadentate Ligand AAZTA. *Chem. - A Eur. J.* 2009, *15* (7), 1696–1705.

(18) Baranyai, Z.; Botta, M.; Fekete, M.; Giovenzana, G. B.; Negri, R.; Tei, L.; Platas-Iglesias, C. Lower Ligand Denticity Leading to Improved Thermodynamic and Kinetic Stability of the Gd 3+ Complex: The Strange Case of OBETA. *Chem. - A Eur. J.* 2012, *18* (25), 7680–7685.

(19) Negri, R.; Baranyai, Z.; Tei, L.; Giovenzana, G. B.; Platas-Iglesias, C.; Bényei, A. C.; Bodnár, J.; Vágner, A.; Botta, M. Lower Denticity Leading to Higher Stability: Structural and Solution Studies of Ln(III)-OBETA Complexes. *Inorg. Chem.* 2014, *53* (23), 12499–12511.

(20) Rodríguez-Rodríguez, A.; Esteban-Gómez, D.; Tripier, R.; Tircsó, G.; Garda, Z.; Tóth, I.; De Blas, A.; Rodríguez-Blas, T.; Platas-Iglesias, C. Lanthanide(III) Complexes with a Reinforced Cyclam Ligand Show Unprecedented Kinetic Inertness. *J. Am. Chem. Soc.* 2014, *136*, 17954–17957.

(21) Aime, S.; Botta, M.; Crich, S. G.; Giovenzana, G. B.; Jommi, G.; Pagliarin, R.; Sisti, M. Synthesis and NMR Studies of Three Pyridine-Containing Triaza Macrocyclic Triacetate Ligands and Their Complexes with Lanthanide Ions. *Inorg. Chem.* 1997, *36* (14), 2992–3000.

(22) Aime, S.; Botta, M.; Geninatti Crich, S.; Giovenzana, G. B.; Jommi, G.; Pagliarin, R.; Sisti, M. MRI Contrast Agents: Macrocyclic Lanthanide(Iii1 Complexes with Improved Relaxation Efficiency. *J. Chem. Soc., Chem. Commun.* 1995, *18*, 1885–1886.

(23) Do, Q. N.; Ratnakar, J. S.; Kovács, Z.; Tircsó, G.; Kálmán, F. K.; Baranyai, Z.; Brücher, E.; Tóth, I. General Synthetic and Physical Methods. In *Contrast Agents for MRI: Experimental Methods*; Valérie C Pierre, M. J. A., Ed.; The Royal Society of Chemistry, 2018; pp 1–120.

(24) Tircsó, G.; Kovács, Z.; Sherry, A. D. Equilibrium and Formation/Dissociation Kinetics of Some Ln IIIPCTA Complexes. *Inorg. Chem.* 2006, *45* (23), 9269–9280.

(25) Aime, S.; Botta, M.; Frullano, L.; Crich, S. G.; Giovenzana, G.; Pagliarin, R.; Palmisano, G.; Sirtori, F. R.; Sisti, M. [GdPCP2A(H2O)2]-: A Paramagnetic Contrast Agent Designed for Improved Applications in Magnetic Resonance Imaging. *J. Med. Chem.* 2000, *43* (21), 4017–4024.

(26) Moreau, J.; Pierrard, J. C.; Rimbault, J.; Guillon, E.; Port, M.; Aplincourt, M. Thermodynamic and Structural Properties of Eu3+complexes of a New 12-Membered Tetraaza Macrocycle Containing Pyridine and N-Glutaryl Groups as Pendant Arms: Characterization of Three Complexing Successive Phases. *Dalt. Trans.* 2007, No. 16, 1611–1620.

(27) Costa, J.; Delgado, R. Metal Complexes of Macrocyclic Ligands Containing Pyridine. *Inorg. Chem.* 1993, *32* (23), 5257–5265.

(28) Leygue, N.; Enel, M.; Diallo, A.; Mestre-Voegtlé, B.; Galaup, C.; Picard, C. Efficient Synthesis of a Family of Bifunctional Chelators Based on the PCTA[12] Macrocycle Suitable for Bioconjugation. *European J. Org. Chem.* 2019, *2019* (18), 2899–2913.

(29) Aime, S.; Botta, M.; Frullano, L.; Crich, S. G.; Giovenzana, G. B.; Pagliarin, R.; Palmisano, G.; Sisti, M. Contrast Agents for Magnetic Resonance Imaging: A Novel Route to Enhanced Relaxivities Based on the Interaction of a Gd(III) Chelate with Poly-β-Cyclodextrins. *Chem. - A Eur. J.* 1999, *5* (4), 1253–1260.

(30) Hovland, R.; Gløgård, C.; Aasen, A. J.; Klaveness, J. Preparation and in Vitro Evaluation of a Novel Amphiphilic GdPCTA-[12] Derivative; a Micellar MRI Contrast Agent. *Org. Biomol. Chem.* 2003, *1* (4), 644–647.

(31) Hao, J.; Bourrinet, P.; Desché, P. Assessment of Pharmacokinetic, Pharmacodynamic Profile, and Tolerance of Gadopiclenol, A New High Relaxivity GBCA, in Healthy Subjects and Patients with Brain Lesions (Phase I/IIa Study). *Invest. Radiol.* 2019, *54* (7), 396–402.

(32) Robic, C.; Port, M.; Rousseaux, O.; Louguet, S.; Fretellier, N.; Catoen, S.; Factor, C.; Le Greneur, S.; Medina, C.; Bourrinet, P.; et al. Physicochemical and Pharmacokinetic Profiles of Gadopiclenol: A New Macrocyclic Gadolinium Chelate With High T1 Relaxivity. *Invest. Radiol.* 2019, *54* (8), 475–484.

(33) Lowe, M. P.; Parker, D.; Reany, O.; Aime, S.;

Botta, M.; Castellano, G.; Gianolio, E.; Pagliarin, R. PH-Dependent Modulation of Relaxivity and Luminescence in Macrocyclic Gadolinium and Europium Complexes Based on Reversible Intramolecular Sulfonamide Ligation. *J. Am. Chem. Soc.* 2001, *123* (31), 7601–7609.

(34) Vologdin, N.; Rolla, G. A.; Botta, M.; Tei, L. Orthogonal Synthesis of a Heterodimeric Ligand for the Development of the GdIII-GaIII Ditopic Complex as a Potential PH-Sensitive MRI/PET Probe. *Org. Biomol. Chem.* 2013, *11* (10), 1683–1690.

(35) Baranyai, Z.; Rolla, G. A.; Negri, R.; Forgács, A.; Giovenzana, G. B.; Tei, L. Comprehensive Evaluation of the Physicochemical Properties of Ln III Complexes of Aminoethyl-DO3A as PH-Responsive T1-MRI Contrast Agents. *Chem. - A Eur. J.* 2014, *20* (10), 2933–2944.

(36) Woods, M.; Kiefer, G. E.; Bott, S.; Castillo-Muzquiz, A.; Eshelbrenner, C.; Michaudet, L.; McMillan, K.; Mudigunda, S. D. K.; Ogrin, D.; Tircsó, G.; et al. Synthesis, Relaxometric and Photophysical Properties of a New PH-Responsive MRI Contrast Agent: The Effect of Other Ligating Groups on Dissociation of a p-Nitrophenolic Pendant Arm. *J. Am. Chem. Soc.* 2004, *126* (30), 9248–9256.

(37) Charbonnière, L. J.; Charpentier, C.; Salaam, J.; Nonat, A.; Carniato, fabio; Jeannin, O.; Brandariz, isabel; Esteban-Gomez, D.; Platas-Iglesias, C.; Botta, M. PH Dependent Hydration Change in a Gd Based MRI Contrast Agent with a Phosphonated Ligand. *Chem. – A Eur. J.* 2020, *n/a* (n/a).

(38) Li, W. H.; Parigi, G.; Fragai, M.; Luchinat, C.; Meade, T. J. Mechanistic Studies of a Calcium-Dependent MRI Contrast Agent. *Inorg. Chem.* 2002, *41* (15), 4018–4024.

(39) Li, W. H.; Fraser, S. E.; Meade, T. J. A Calcium-Sensitive Magnetic Resonance Imaging Contrast Agent [18]. *J. Am. Chem. Soc.* 1999, *121* (6), 1413–1414.

(40) Angelovski, G.; Chauvin, T.; Pohmann, R.; Logothetis, N. K.; Tóth, É. Calcium-Responsive Paramagnetic CEST Agents. *Bioorganic Med. Chem.* 2011, *19* (3), 1097–1105.

(41) Que, E. L.; Gianolio, E.; Baker, S. L.; Aime, S.; Chang, C. J. A Copper-Activated Magnetic Resonance Imaging Contrast Agent with Improved Turn-on Relaxivity Response and Anion Compatibility. *Dalt. Trans.* 2010, *39* (2), 469–476.

(42) Que, E. L.; Gianolio, E.; Baker, S. L.; Wong, A. P.; Aime, S.; Chang, C. J. Copper-Responsive Magnetic Resonance Imaging Contrast Agents. *J. Am. Chem. Soc.* 2009, *131* (24), 8527–8536.

(43) Kadjane, P.; Platas-Iglesias, C.; Boehm-Sturm, P.; Truffault, V.; Hagberg, G. E.; Hoehn, M.; Logothetis, N. K.; Angelovski, G. Dual-Frequency Calcium-Responsive MRI Agents. *Chem. - A Eur. J.* 2014, *20* (24), 7351–7362.

(44) Jordan, M. V. C.; Lo, S. T.; Chen, S.; Preihs, C.; Chirayil, S.; Zhang, S.; Kapur, P.; Li, W. H.; De Leon-Rodriguez, L. M.; Lubag, A. J. M.; et al. Zinc-Sensitive MRI Contrast Agent Detects Differential Release of Zn(II) Ions from the Healthy vs. Malignant Mouse Prostate. *Proc. Natl. Acad. Sci. U. S. A.* 2016, *113* (37), E5464–E5471.

(45) Esqueda, A. C.; López, J. A.; Andreu-de-Riquer, G.; Alvarado-Monzón, J. C.; Ratnakar, J.; Lubag, A. J. M.; Sherry, A. D.; De León-Rodríguez, L. M. A New Gadolinium-Based MRI Zinc Sensor. *J. Am. Chem. Soc.* 2009, *131* (32), 11387–11391.

(46) Yu, J.; Martins, A. F.; Preihs, C.; Clavijo Jordan, V.; Chirayil, S.; Zhao, P.; Wu, Y.; Nasr, K.; Kiefer, G. E.; Sherry, A. D. Amplifying the Sensitivity of Zinc(II) Responsive MRI Contrast Agents by Altering Water Exchange Rates. *J. Am. Chem. Soc.* 2015, *137* (44), 14173–14179.

(47) Regueiro-Figueroa, M.; Gündüz, S.; Patinec, V.; Logothetis, N. K.; Esteban-Gómez, D.; Tripier, R.; Angelovski, G.; Platas-Iglesias, C. Gd^{3+}-Based Magnetic Resonance Imaging Contrast Agent Responsive to Zn2+. *Inorg. Chem.* 2015, *54* (21), 10342–10350.

(48) Abada, S.; Lecointre, A.; Elhabiri, M.; Esteban-Gómez, D.; Platas-Iglesias, C.; Tallec, G.; Mazzanti, M.; Charbonnière, L. J. Highly Relaxing Gadolinium Based MRI Contrast Agents Responsive to Mg 2+ Sensing. *Chem. Commun.* 2012, *48* (34), 4085–4087.

(49) Gündüz, S.; Nitta, N.; Vibhute, S.; Shibata, S.; Mayer, M. E.; Logothetis, N. K.; Aoki, I.; Angelovski, G. Dendrimeric Calcium-Responsive MRI Contrast Agents with Slow in Vivo Diffusion. *Chem. Commun.* 2015, *51* (14), 2782–2785.

(50) Angelovski, G.; Tóth, É. Strategies for Sensing

Neurotransmitters with Responsive MRI Contrast Agents. *Chem. Soc. Rev.* 2017, *46* (2), 324–336.

(51) Oukhatar, F.; Eliseeva, S. V.; Bonnet, C. S.; Placidi, M.; Logothetis, N. K.; Petoud, S.; Angelovski, G.; Tóth, É. Toward MRI and Optical Detection of Zwitterionic Neurotransmitters: Near-Infrared Luminescent and Magnetic Properties of Macrocyclic Lanthanide(III) Complexes Appended with a Crown Ether and a Benzophenone Chromophore. *Inorg. Chem.* 2019, *58* (20), 13619–13630.

(52) Oukhatar, F.; Même, S.; Même, W.; Szeremeta, F.; Logothetis, N. K.; Angelovski, G.; Tóth, É. MRI Sensing of Neurotransmitters with a Crown Ether Appended Gd3+ Complex. *ACS Chem. Neurosci.* 2015, *6* (2), 219–225.

(53) Toljić, Đ.; Platas-Iglesias, C.; Angelovski, G. In-Depth Study of a Novel Class of Ditopic Gadolinium(III)-Based MRI Probes Sensitive to Zwitterionic Neurotransmitters. *Front. Chem.* 2019, *7* (July), 1–12.

(54) Duimstra, J. A.; Femia, F. J.; Meade, T. J. A Gadolinium Chelate for Detection of β-Glucuronidase: A Self-Immolative Approach. *J. Am. Chem. Soc.* 2005, *127* (37), 12847–12855.

(55) Urbanczyk-Pearson, L. M.; Femia, F. J.; Smith, J.; Parigi, G.; Duimstra, J. A.; Eckermann, A. L.; Luchinat, C.; Meade, T. J. Mechanistic Investigation of β-Galactosidase-Activated MR Contrast Agents. *Inorg. Chem.* 2008, *47* (1), 56–68.

(56) Chauvin, T.; Durand, P.; Bernier, M.; Meudal, H.; Doan, B. T.; Noury, F.; Badet, B.; Beloeil, J. C.; Tóth, É. Detection of Enzymatic Activity by PARACEST MRI: A General Approach to Target a Large Variety of Enzymes. *Angew. Chemie - Int. Ed.* 2008, *47* (23), 4370–4372.

(57) Pinto, S. M.; Tomé, V.; Calvete, M. J. F.; Castro, M. M. C. A.; Tóth, É.; Geraldes, C. F. G. C. Metal-Based Redox-Responsive MRI Contrast Agents. *Coord. Chem. Rev.* 2019, *390*, 1–31.

(58) Tsitovich, P. B.; Burns, P. J.; McKay, A. M.; Morrow, J. R. Redox-Activated MRI Contrast Agents Based on Lanthanide and Transition Metal Ions. *J. Inorg. Biochem.* 2014, *133*, 143–154.

(59) Basal, L. A.; Bailey, M. D.; Romero, J.; Ali, M. M.; Kurenbekova, L.; Yustein, J.; Pautler, R. G.; Allen, M. J. Fluorinated Eu II -Based Multimodal Contrast Agent for Temperature- and Redox-Responsive Magnetic Resonance Imaging. *Chem. Sci.* 2017, *8* (12), 8345–8350.

(60) Burnett, M. E.; Adebesin, B.; Funk, A. M.; Kovacs, Z.; Sherry, A. D.; Ekanger, L. A.; Allen, M. J.; Green, K. N.; Ratnakar, S. J. Electrochemical Investigation of the Eu3+/2+ Redox Couple in Complexes with Variable Numbers of Glycinamide and Acetate Pendant Arms. *Eur. J. Inorg. Chem.* 2017, *2017* (43), 5001–5005.

(61) Loving, G. S.; Mukherjee, S.; Caravan, P. Redox-Activated Manganese-Based MR Contrast Agent. *J. Am. Chem. Soc.* 2013, *135* (12), 4620–4623.

(62) Funk, A. M.; Clavijo Jordan, V.; Sherry, A. D.; Ratnakar, S. J.; Kovacs, Z. Oxidative Conversion of a Europium(II)-Based T1 Agent into a Europium(III)-Based ParaCEST Agent That Can Be Detected in Vivo by Magnetic Resonance Imaging. *Angew. Chemie - Int. Ed.* 2016, *55* (16), 5024–5027.

(63) Ratnakar, S. J.; Viswanathan, S.; Kovacs, Z.; Jindal, A. K.; Green, K. N.; Sherry, A. D. Europium(III) Dota-Tetraamide Complexes as Redox-Active Mri Sensors. *J. Am. Chem. Soc.* 2012, *134* (13), 5798–5800.

(64) Hao, G.; Xu, Z. P.; Li, L. Manipulating Extracellular Tumour PH: An Effective Target for Cancer Therapy. *RSC Adv.* 2018, *8* (39), 22182–22192.

(65) Casimir, G. J.; Lefèvre, N.; Corazza, F.; Duchateau, J.; Chamekh, M. The Acid-Base Balance and Gender in Inflammation: A Mini-Review. *Front. Immunol.* 2018, *9* (MAR), 1–6.

(66) Aime, S.; Fedeli, F.; Sanino, A.; Terreno, E. A R2/R1 Ratiometric Procedure for a Concentration-Independent, pH-Responsive, Gd(III)-Based MRI Agent. *J. Am. Chem. Soc.* 2006, *128* (35), 11326–11327.

(67) Kim, W. D.; Kiefer, G. E.; Maton, F.; McMillan, K.; Muller, R. N.; Dean Sherry, A. Relaxometry, Luminescence Measurements, Electrophoresis, and Animal Biodistribution of Lanthanide(III) Complexes of Some Polyaza Macrocyclic Acetates Containing Pyridine. *Inorg. Chem.* 1995, *34* (8), 2233–2243.

(68) Le Fur, M.; Molnár, E.; Beyler, M.; Fougère, O.; Esteban-Gómez, D.; Rousseaux, O.; Tripier, R.;

Tircsó, G.; Platas-Iglesias, C. Expanding the Family of Pyclen-Based Ligands Bearing Pendant Picolinate Arms for Lanthanide Complexation. *Inorg. Chem.* 2018, *57* (12), 6932–6945.

(69) Le Fur, M.; Molnár, E.; Beyler, M.; Kálmán, F. K.; Fougère, O.; Esteban-Gómez, D.; Rousseaux, O.; Tripier, R.; Tircsó, G.; Platas-Iglesias, C. A Coordination Chemistry Approach to Fine-Tune the Physicochemical Parameters of Lanthanide Complexes Relevant to Medical Applications. *Chem. - A Eur. J.* 2018, *24* (13), 3127–3131.

(70) Marín, C.; Clares, M. P.; Ramírez-Macías, I.; Blasco, S.; Olmo, F.; Soriano, C.; Verdejo, B.; Rosales, M. J.; Gomez-Herrera, D.; García-España, E.; et al. In Vitro Activity of Scorpiand-like Azamacrocycle Derivatives in Promastigotes and Intracellular Amastigotes of Leishmania Infantum and Leishmania Braziliensis. *Eur. J. Med. Chem.* 2013, *62*, 466–477.

(71) Pont, I.; González-García, J.; Inclán, M.; Reynolds, M.; Delgado-Pinar, E.; Albelda, M. T.; Vilar, R.; García-España, E. Aza-Macrocyclic Triphenylamine Ligands for G-Quadruplex Recognition. *Chem. – A Eur. J.* 2018, *24* (42), 10850–10858.

(72) Kim, W. D.; Hrncir, D. C.; Kiefer, G. E.; Dean Sherry, A. Synthesis, Crystal Structure, and Potentiometry of Pyridine-Containing Tetraaza Macrocyclic Ligands with Acetate Pendant Arms. *Inorg. Chem.* 1995, *34* (8), 2225–2232.

(73) Aime, S.; Gianolio, E.; Corpillo, D.; Cavallotti, C.; Palmisano, G.; Sisti, M.; Giovenzana, G. B.; Pagliarin, R. Designing Novel Contrast Agents for Magnetic Resonance Imaging. Synthesis and Relaxometric Characterization of Three Gadolinium(III) Complexes Based on Functionalized Pyridine-Containing Macrocyclic Ligands. *Helv. Chim. Acta* 2003, *86* (3), 615–632.

(74) Platas, C.; Avecilla, F.; de Blas, A.; Rodriguez-Blas, T.; Geraldes, C. F. G. C.; Tóth, É.; Merbach, A. E.; Bünzli, J. C. G. Mono- and Bimetallic Lanthanide(Ni) Phenolic Cryptâtes Obtained by Template Reaction: Solid State Structure, Photophysical Properties and Relaxivity. *J. Chem. Soc. Dalt. Trans.* 2000, No. 4, 611–618.

(75) Aime, S.; Cavallotti, C.; Gianolio, E.; Giovenzana, G. B.; Palmisano, G.; Sisti, M. Mannich Reaction as a New Route to Pyridine-Based Polyaminocarboxylic Ligands. *Org. Lett.* 2004, *6* (8), 1201–1204.

(76) Aime, S.; Botta, M.; Esteban-Gómez, D.; Platas-Iglesias, C. Characterisation of Magnetic Resonance Imaging (MRI) Contrast Agents Using NMR Relaxometry. *Mol. Phys.* 2019, *117* (7–8), 898–909.

(77) Binnemans, K. Interpretation of Europium(III) Spectra. *Coord. Chem. Rev.* 2015, *295*, 1–45.

(78) Werts, M. H. V.; Jukes, R. T. F.; Verhoeven, J. W. The Emission Spectrum and the Radiative Lifetime of Eu3+ in Luminescent Lanthanide Complexes. *Phys. Chem. Chem. Phys.* 2002, *4* (9), 1542–1548.

(79) Di Bari, L.; Pintacuda, G.; Salvadori, P.; Dickins, R. S.; Parker, D. Effect of Axial Ligation on the Magnetic and Electronic Properties of Lanthanide Complexes of Octadentate Ligands. *J. Am. Chem. Soc.* 2000, *122* (38), 9257–9264.

(80) Dickins, R. S.; Parker, D.; Bruce, J. I.; Tozer, D. J. Correlation of Optical and NMR Spectral Information with Coordination Variation for Axially Symmetric Macrocyclic Eu(III) and Yb(III) Complexes: Axial Donor Polarisability Determines ligand Field and Cation Donor Preference. *Dalt. Trans.* 2003, No. 7, 1264–1271.

(81) Murray, B. S.; New, E. J.; Pal, R.; Parker, D. Critical Evaluation of Five Emissive Europium(III) Complexes as Optical Probes: Correlation of Cytotoxicity, Anion and Protein Affinity with Complex Structure, Stability and Intracellular Localisation Profile. *Org. Biomol. Chem.* 2008, *6* (12), 2085–2094.

(82) Gündüz, S.; Vibhute, S.; Botár, R.; Kálmán, F. K.; Tóth, I.; Tircsó, G.; Regueiro-Figueroa, M.; Esteban-Gómez, D.; Platas-Iglesias, C.; Angelovski, G. Coordination Properties of GdDO3A-Based Model Compounds of Bioresponsive MRI Contrast Agents. *Inorg. Chem.* 2018, *57* (10), 5973–5986.

(83) Supkowski, R. M.; Horrocks, W. D. J. On the Determination of the Number of Water Molecules, q, Coordinated to Europium(III) Ions in Solution from Luminescence Decay Lifetimes. *Inorganica Chim. Acta* 2002, *340* (0), 44–48.

(84) Beeby, A.; Clarkson, I. M.; Dickins, R. S.; Faulkner, S.; Parker, D.; Royle, L.; De Sousa, A. S.; Williams, J. A. G.; Woods, M. Non-Radiative Deactivation of the Excited States of Europium, Terbium and

Ytterbium Complexes by Proximate Energy-Matched OH, NH and CH Oscillators: An Improved Luminescence Method for Establishing Solution Hydration States. *J. Chem. Soc. Perkin Trans. 2* 1999, *2* (3), 493–503.

(85) Aime, S.; Botta, M.; Crich, S. G.; Giovenzana, G.; Pagliarin, R.; Sisti, M.; Terreno, E. NMR Relaxometric Studies of Gd(III) Complexes with Heptadentate Macrocyclic Ligands. *Magn. Reson. Chem.* 1998, *36* (S1), S200–S208.

(86) Powell, D. H.; Ni Dhubhghaill, O. M.; Pubanz, D.; Helm, L.; Lebedev, Y. S.; Schlaepfer, W.; Merbach, A. E. Structural and Dynamic Parameters Obtained from 17O NMR, EPR, and NMRD Studies of Monomeric and Dimeric Gd3+ Complexes of Interest in Magnetic Resonance Imaging: An Integrated and Theoretically Self-Consistent Approach. *J. Am. Chem. Soc.* 1996, *118* (39), 9333–9346.

(87) Peters, J. A. The Reliability of Parameters Obtained by Fitting of 1H NMRD Profiles and 17O NMR Data of Potential Gd3+-Based MRI Contrast Agents. *Contrast Media Mol. Imaging* 2016, *11* (2), 160–168.

(88) Maigut, J.; Meier, R.; Zahl, A.; Van Eldik, R. Triggering Water Exchange Mechanisms via Chelate Architecture. Shielding of Transition Metal Centers by Aminopolycarboxylate Spectator Ligands. *J. Am. Chem. Soc.* 2008, *130* (44), 14556–14569.

(89) Balogh, E.; Mato-Iglesias, M.; Platas-Iglesias, C.; Tóth, É.; Djanashvili, K.; Peters, J. A.; De Blas, A.; Rodríguez-Blas, T. Pyridine- and Phosphonate-Containing Ligands for Stable Ln Complexation. Extremely Fast Water Exchange on the GdIII Chelates. *Inorg. Chem.* 2006, *45* (21), 8719–8728.

(90) Astashkin, A. V.; Raitsimring, A. M.; Caravan, P. Pulsed ENDOR Study of Water Coordination to Gd3+ Complexes in Orientationally Disordered Systems. *J. Phys. Chem. A* 2004, *108* (11), 1990–2001.

(91) Borel, A.; Helm, L.; Merbach, A. E. Molecular Dynamics Simulations of MRI-Relevant GdIII Chelates: Direct Access to Outer-Sphere Relaxivity. *Chem. - A Eur. J.* 2001, *7* (3), 600–610.

(92) Elst, L. Vander; Sessoye, A.; Laurent, S.; Muller, R. N. Can the Theoretical Fitting of the Proton-Nuclear-Magnetic-Relaxation- Dispersion (Proton NMRD) Curves of Paramagnetic Complexes Be Improved by Independent Measurement of Their Self-Diffusion Coefficients? *Helv. Chim. Acta* 2005, *88* (3), 574–587.

(93) Lammers, H.; Maton, F.; Pubanz, D.; Van Laren, M. W.; Van Bekkum, H.; Merbach, A. E.; Muller, R. N.; Peters, J. A. Structures and Dynamics of Lanthanide(III) Complexes of Sugar-Based DTP A-Bis (Amides) in Aqueous Solution: A Multinuclear NMR Study. *Inorg. Chem.* 1997, *36* (12), 2527–2538.

(94) Esteban-Gómez, D.; de Blas, A.; Rodríguez-Blas, T.; Helm, L.; Platas-Iglesias, C. Hyperfine Coupling Constants on Inner-Sphere Water Molecules of Gd(III)-Based MRI Contrast Agents. *Chemphyschem* 2012, *13* (16), 3640–3650.

(95) Yazyev, O. V.; Helm, L.; Malkin, V. G.; Malkina, O. L. Quantum Chemical Investigation of Hyperfine Coupling Constants on First Coordination Sphere Water Molecule of Gadolinium(III) Aqua Complexes. *J. Phys. Chem. A* 2005, *109* (48), 10997–11005.

(96) Miéville, P.; Jannin, S.; Helm, L.; Bodenhausen, G. Kinetics of Yttrium-Ligand Complexation Monitored Using Hyperpolarized 89Y as a Model for Gadolinium in Contrast Agents. *J. Am. Chem. Soc.* 2010, *132* (14), 5006–5007.

(97) Regueiro-Figueroa, M.; Platas-Iglesias, C. Toward the Prediction of Water Exchange Rates in Magnetic Resonance Imaging Contrast Agents: A Density Functional Theory Study. *J. Phys. Chem. A* 2015, *119* (24), 6436–6445.

(98) Krchová, T.; Herynek, V.; Gálisová, A.; Blahut, J.; Hermann, P.; Kotek, J. Eu(III) Complex with DO3A-Amino-Phosphonate Ligand as a Concentration-Independent PH-Responsive Contrast Agent for Magnetic Resonance Spectroscopy (MRS). *Inorg. Chem.* 2017, *56* (4), 2078–2091.

(99) Regueiro-Figueroa, M.; Nonat, A.; Rolla, G. A.; Esteban-Gõmez, D.; De Blas, A.; Rodríguez-Blas, T.; Charbonnière, L. J.; Botta, M.; Platas-Iglesias, C. Self-Aggregated Dinuclear Lanthanide(III) Complexes as Potential Bimodal Probes for Magnetic Resonance and Optical Imaging. *Chem. - A Eur. J.* 2013, *19* (35), 11696–11706.

(100) Costa, J.; Balogh, E.; Turcry, V.; Tripier, R.; Le Baccon, M.; Chuburu, F.; Handel, H.; Helm, L.; Tóth, E.; Merbach, A. E. Unexpected Aggregation of Neutral, Xylene-Cored Dinuclear GdIII Chelates in Aqueous Solution. *Chem. Eur. J.*

2006, *12* (26), 6841–6851.

(101) Rodríguez-Rodríguez, A.; Garda, Z.; Ruscsák, E.; Esteban-Gómez, D.; De Blas, A.; Rodríguez-Blas, T.; Lima, L. M. P.; Beyler, M.; Tripier, R.; Tircsó, G.; et al. Stable Mn2+, Cu2+ and Ln3+ Complexes with Cyclen-Based Ligands Functionalized with Picolinate Pendant Arms. *Dalt. Trans.* 2015, *44* (11), 5017–5031.

(102) Wacker, A.; Carniato, F.; Platas-Iglesias, C.; Esteban-Gomez, D.; Wester, H. J.; Tei, L.; Notni, J. Dimer Formation of GdDO3A-Arylsulfonamide Complexes Causes Loss of PH-Dependency of Relaxivity. *Dalt. Trans.* 2017, *46* (48), 16828–16836.

(103) Dolomanov, O. V.; Bourhis, L. J.; Gildea, R. J.; Howard, J. A. K.; Puschmann, H. OLEX2: A Complete Structure Solution, Refinement and Analysis Program. *J. Appl. Crystallogr.* 2009, *42* (2), 339–341.

(104) Burla, M. C.; Caliandro, R.; Carrozzini, B.; Cascarano, G. L.; Cuocci, C.; Giacovazzo, C.; Mallamo, M.; Mazzone, A.; Polidori, G. Crystal Structure Determination and Refinement via SIR2014. *J. Appl. Crystallogr.* 2015, *48* (1), 306–309.

(105) Sheldrick, G. M. Crystal Structure Refinement with SHELXL. *Acta Crystallogr. Sect. C Struct. Chem.* 2015, *71* (Md), 3–8.

(106) Frisch, M. J.; Trucks, G. W.; Schlegel, H. B.; Scuseria, G. E.; Robb, M. A.; Cheeseman, J. R.; Scalmani, G.; Barone, V.; Petersson, G. A.; Nakatsuji, H.; et al. Gaussian 09. Gaussian, Inc.: Wallingford CT 2009.

(107) Tao, J.; Perdew, J. P.; Staroverov, V. N.; Scuseria, G. E. Climbing the Density Functional Ladder: Nonempirical Meta–Generalized Gradient Approximation Designed for Molecules and Solids. *Phys. Rev. Lett.* 2003, *91* (14), 146401-1-146401–146404.

(108) Tomasi, J.; Mennucci, B.; Cammi, R. Quantum Mechanical Continuum Solvation Models. *Chem. Rev.* 2005, *105* (8), 2999–3093.

(109) Dolg, M.; Stoll, H.; Savin, A.; Preuss, H. Energy-Adjusted Pseudopotentials for the Rare Earth Elements. *Theor. Chim. Acta* 1989, *75* (3), 173–194.

TOC Graphic:

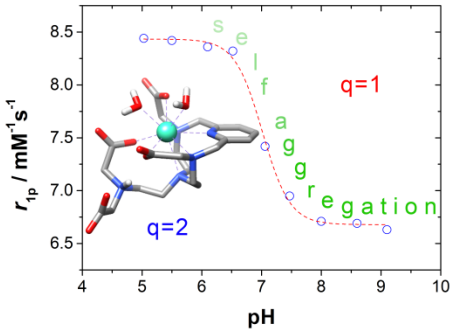

A new Gd^{3+} complex with a scorpiand ligand exhibits an interesting relaxivity pH response associated with a change in the number of water molecules coordinated to the metal ion. Deprotonation of the ligand allows intermolecular coordination and formation of small aggregates, resulting in a reduced hydration number.